PHYSICAL REVIEW B VOLUME 27, NUMBER 6 15 MARCH 1983

Lattice dynamics of fcc Ca

C. Stassis, J. Zaretsky, D. K. Misemer, H. L. Skriver,* and B. N. Harmon
Ames Laboratory and Department of Physics, Iowa State University, Ames, Iowa 50011

R. M. Nicklow
Solid State Division, Oak Ridge National Laboratory, Oak Ridge, Tennessee 37830
(Received 18 October 1982)

A large single crystal of fcc Ca was grown and was used to study the lattice dynamics of this divalent metal by coherent inelastic neutron scattering. The phonon dispersion curves were measured, at room temperature, along the $[\xi 00]$, $[\xi\xi 0]$, $[\xi\xi\xi]$, and $[0\xi 1]$ symmetry directions. The dispersion curves bear a striking resemblance to those of fcc Yb, which is also a divalent metal with an electronic band structure similar to that of Ca. In particular, the shear moduli c_{44} and $(c_{11}-c_{12})/2$ differ by a factor of 3.4, which implies that fcc Ca (like fcc Yb) is very anisotropic with regard to the propagation of elastic waves. The frequencies of the $T_1[\xi\xi 0]$ branch for ξ between approximately 0.5 and 0.8 are slightly above the velocity-of-sound line determined from the low-frequency measurements. Since a similar effect has been observed in fcc Yb, it is natural to assume that the anomalous dispersion exhibited by the $T_1[\xi\xi 0]$ branches of these metals is due to an electronic effect. To provide further support for this assumption we have performed a band theoretical calculation of the generalized susceptibility $\chi(\vec{q})$ of fcc Ca. The results suggest that, for ξ between approximately 0.6 and 0.8, there is a relative decrease in the electronic screening of the vibrational motion of the nuclei, which may account for the positive dispersion exhibited by the $T_1[\xi\xi 0]$ branch in this range of ξ values. The data were used to evaluate the elastic constants, the phonon density of states, and the lattice specific heat of fcc Ca.

I. INTRODUCTION

The alkaline-earth metals Ba, Ca, and Sr, and the rare-earth metals Yb and Eu are all divalent and possess similar physical properties. Under normal conditions of temperature and pressure, Ca, Sr, and Yb are fcc, whereas Ba and Eu are bcc. Of particular interest is the understanding, from a fundamental point of view, of the structure and physical properties of these metals.

A large number of band-structure calculations[1–4] have established quite well the general features of the electronic bands of these divalent metals. Below the Fermi level, the electronic bands are relatively simple and almost free-electron-like. Because of the proximity of the d bands to the Fermi level, however, the electronic wave functions at the Fermi level contain a significant admixture of d character. The position of the d bands relative to the Fermi level, and hence the amount of hybridization, play an important role in determining the physical properties of these metals.

The experimental investigation of the elastic and lattice-dynamical properties of the alkaline-earth metals has been hindered considerably by the difficulty of growing large single crystals of these metals. Recently, however, we were able to grow a single crystal of fcc Ca of sufficient volume for the study of the elastic constants and phonon dispersion curves of this metal. In the present paper we report the results of our measurements of the phonon dispersion curves of fcc Ca.

II. EXPERIMENTAL DETAILS

Polycrystalline samples of high-purity Ca were prepared by arc melting and were encapsulated under helium in thin-wall tantalum crucibles. The tantalum crucibles were mounted on the sample holder of a vacuum neutron-diffraction furnace, which was positioned on the sample goniometer of a conventional double-axis diffractometer. There is a definite advantage in using this experimental arrangement, since various techniques for growing the crystals may be attempted and the success of a particular method can be immediately assessed by standard neutron-diffraction techniques.

The single crystal used in the experiments was grown by the following procedure. A large bcc crystal was first grown from the melt, then an fcc crystal of comparable size (~ 3 cm^3) was obtained by cycling several times through the bcc↔fcc transforma-

tion temperature ($\sim$720 K). The mosaic spread of the crystal has been measured to be approximately 2°. This relatively large mosaic spread complicated the determination of the dispersion curves, especially of the transverse branches. We attempted to improve the mosaic spread of the crystal by annealing at temperatures close to the fcc→bcc transformation temperature. Unfortunately, this annealing had no measurable effect on the mosaic spread of the crystal.

A complete set of measurements of the dispersion curves was obtained using the HB-3 triple-axis spectrometer at the high-flux isotope reactor (HFIR) of the Oak Ridge National Laboratory. Beryllium reflecting from the (002) planes was used as both monochromator and analyzer, and the collimation before and after the sample was 40 min of arc. The data were collected using the constant $\vec{Q}$ (the neutron scattering vector) method, and constant scattered neutron energies of 8, 6, and 3.6 THz (in the latter case a pyrolytic graphite filter was used in the scattered beam to attenuate higher-order contaminations).

The frequencies of the $T_1[\xi\xi 0]$ branch for ξ between approximately 0.5 and 0.8 were found to be slightly above the values expected from measurements at lower frequencies. To verify this point, this branch was also studied systematically using the HB-1A triple-axis spectrometer at the HFIR and a triple-axis spectrometer at the Oak Ridge research reactor (ORR) of the Oak Ridge National Laboratory. The HB-1A spectrometer was operated at a constant incident energy of 3.6 THz (with a pyrolite graphite filter placed after the monochromator), and the monochromator and analyzer were pyrolitic graphite and Be, respectively [both reflecting from the (002) planes]. The ORR spectrometer was operated at a constant scattered neutron energy of 3.6 THz (with a pyrolite graphite filter in the scattered beam) and pyrolitic graphite [reflecting from the (002) planes] was used as both monochromator and analyzer. In both spectrometers the collimation before and after the sample was 40 min of arc. The frequencies of the $T_1[\xi\xi 0]$ measured on all three instruments were found to agree to within experimental precision.

III. EXPERIMENTAL RESULTS AND DISCUSSION

The phonon dispersion curves were measured, at room temperature, along the $[00\xi]$, $[\xi\xi 0]$, $[\xi\xi\xi]$, and $[0\xi 1]$ symmetry directions. The measured phonon frequencies are listed in Table I and the dispersion curves are plotted in Fig. 1. The measured phonon dispersion curves are in quite good agreement with those obtained[5] by Buchenau, Schober, and Wagner from Born–von Kármán force constants, which were determined from the time-of-flight spectrum of a polycrystalline sample.

The dispersion curves of fcc Ca bear a striking resemblance to those[6] of fcc Yb. In particular, notice (Fig. 1) (a) the large difference in the slopes of the $T_1[\xi\xi 0]$ and $T_2[\xi\xi 0]$ branches, which implies that fcc Ca (as Yb) is very anisotropic with regard to the propagation of elastic waves, and (b) the anomalous dispersion exhibited (as in Yb) by the $T_1[\xi\xi 0]$ branch. More generally, the phonon frequencies of Ca are in quite good agreement with those obtained from the Yb frequencies, when the differences in masses, interatomic spacings, and melting temperatures of these metals are taken into account. The similarity between the dispersion curves of these metals is not surprising, since fcc Yb is also a divalent metal with a similar electronic band structure to that of fcc Ca (except that the *d* bands of Yb are slightly lower than those of Ca).

Several theoretical calculations of the dispersion curves of fcc Ca have been performed within the framework of the pseudopotential theory of metals. The phonon frequencies calculated[7] by Animalu, using a local potential, are substantially higher (for some phonon frequencies by as much as 65%) than the experimental values. The phonon frequencies calculated[8] by Taut and Eschrig, using a nonlocal pseudopotential, are in relatively better agreement with the experimental data; the calculated frequencies are lower than the experimental values, with a maximum deviation of approximately 16%. More recently, Moriarty[9] calculated the phonon frequencies of Ca using a pseudopotential approach which takes into account the effects of hybridization with the *d* states. The phonon frequencies calculated[9] by Moriarty are in better agreement with the experiment, especially for the transverse branches, than those obtained[8] by Taut and Eschrig. This implies that the hybridization of the free-electron-like bands with the *d* states near E_F may be quite important in determining the phonon dispersion curves of fcc Ca. Clearly, first-principles frozen phonon calculations[10] could provide additional information. In such calculations the effects of the electronic screening on the vibrational motion of the nuclei can be studied in detail for particular phonons to assess the importance of the hybridization involving the *d* bands near E_F. Unfortunately, such calculations are not presently available.

A rather interesting aspect of the dispersion curves of fcc Ca is the anomalous dispersion exhibited by the $T_1[\xi\xi 0]$ branch (see Fig. 1). The frequencies of this branch for ξ between approximately 0.5 and 0.8 are slightly above the velocity-of-sound line

TABLE I. Measured phonon frequencies (THz) of fcc Ca.

ξ	ν	ξ	ν	ξ	ν
	[00ξ]L		[00ξ]T		[$\xi\xi\xi$]L
0.2	1.50±0.04	0.15	0.83±0.04	0.1	1.60±0.08
0.3	2.28±0.06	0.2	1.07±0.10	0.15	2.32±0.06
0.4	3.17±0.08	0.3	1.69±0.10	0.2	2.90±0.10
0.5	3.66±0.10	0.4	2.28±0.04	0.25	3.34±0.06
0.6	4.13±0.08	0.5	2.54±0.05	0.3	3.90±0.14
0.7	4.35±0.08	0.6	2.92±0.06	0.4	4.51±0.12
0.8	4.40±0.06	0.7	3.29±0.04	0.5	4.61±0.08
0.9	4.59±0.08	0.8	3.42±0.04		
1.0	4.52±0.08	0.9	3.61±0.03		
		1.0	3.63±0.06		
	[$\xi\xi\xi$]T		[$\xi\xi$0]L		[$\xi\xi$0]T_2
0.2	1.26±0.04	0.1	1.29±0.04	0.3	2.42±0.09
0.3	1.81±0.05	0.15	1.78±0.04	0.4	2.91±0.03
0.4	2.16±0.04	0.2	2.44±0.03	0.5	3.50±0.07
0.5	2.36±0.06	0.3	3.22±0.04	0.6	4.14±0.04
		0.4	3.94±0.04	0.7	4.39±0.04
	[$\xi\xi$0]T_1	0.5	4.14±0.10	0.8	4.61±0.03
0.2	0.80±0.04	0.6	4.19±0.05	0.9	4.70±0.03
0.3	1.15±0.04	0.7	4.04±0.04	1.0	4.62±0.04
0.4	1.64±0.04	0.8	3.84±0.06		
0.5	2.01±0.08	0.9	3.68±0.06		
0.6	2.63±0.03		[0ξ1]Λ		[0ξ1]Π
0.7	3.02±0.03	0.1	3.64±0.06	0.2	4.62±0.04
0.8	3.14±0.10	0.2	3.50±0.06	0.4	4.42±0.06
0.9	3.30±0.08	0.3	3.29±0.06	0.6	4.16±0.08
1.0	3.63±0.06	0.4	3.09±0.06	0.8	3.79±0.03
		0.5	2.89±0.09		

determined from the low ξ measurements (positive dispersion). This positive dispersion of the $T_1[\xi\xi 0]$ branch was verified by systematic measurements performed on three different spectrometers (see Sec. II). A similar effect has been observed,[6] as we have already mentioned, in fcc Yb. Since both Ca and Yb are divalent, with quite similar electronic band structures, it is natural to assume that the positive dispersion exhibited by the $T_1[\xi\xi 0]$ branches of these metals is due to an electronic effect.

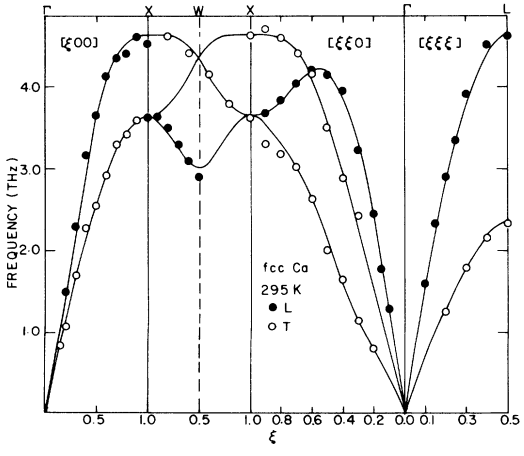

FIG. 1. Experimental dispersion curves of fcc Ca. The solid lines were obtained by fitting the data to an eight-nearest-neighbor force-constant model.

Phonon anomalies and their relation to the electronic structure of metals have been studied extensively[11] within the framework of linear response theory. Information about the position, and often the shape of the phonon anomalies, is contained in the generalized susceptibility function $\chi(\vec{q})$, which is the electronic response to changes in the crystal potential due to the lattice vibrations. Consequently, following customary procedures,[11] we have evaluated $\chi(\vec{q})$ along the [110] direction assuming constant matrix elements, to ascertain whether any features of this function can be correlated with the observed phonon anomaly. The self-consistent band structure of Ca was calculated[4] using the linear muffin-tin orbital (LMTO) technique. Energy eigenvalues were determined at 240 $\vec{k}$ points in the irreducible zone. In order to interpolate between these points, each band was represented by a Fourier

series consisting of 60 symmetrized plane waves. The coefficients of the series were determined by a least-squares fit, with an rms error of less than 2 mRy. The Fourier representation was then used to generate energy eigenvalues at the corners of 2048 tetrahedra. Within each tetrahedron, the energy was linearly interpolated, and the susceptibility evaluated by standard techniques.[12] It can be seen (Fig. 2) that for ξ between approximately 0.6 and 0.8 the generalized susceptibility for bands 1 and 2 exhibits a rather abrupt decrease. This relative decrease of the generalized susceptibility results in a less effective electronic screening of the vibrational motion of the nuclei, and may account for the positive dispersion exhibited by the $T_1[\xi\xi 0]$ branch in this range of ξ values. It should be pointed out, however, that a more elaborate calculation[13] (including the electron-phonon matrix elements) is necessary to establish that only the $T_1[110]$ branch (and not the $T_2[110]$ or $L[110]$ branch) is significantly affected by this decrease in the electronic screening, and to estimate the magnitude of the anomaly.

To evaluate the elastic constants and the lattice specific heat, the data were analyzed by conventional Born–von Kármán force-constant models. Models with up to eight-nearest-neighbor atomic force constants were used in analyzing the experimental data. It can be seen (Fig. 1) that the eight-nearest-neighbor force-constant model provides an adequate fit to the experimental data. The force constants obtained by fitting the data, and the elastic constants evaluated using this model, are listed in Table II. No single-crystal measurements of the elastic constants of fcc Ca are presently available to be compared with the results of the present analysis. The values for the elastic constants of fcc Ca obtained in this work are, however, in reasonable agreement with the values obtained[14] by Buchenau

TABLE II. Atomic force constants and elastic constants obtained by fitting the data to an eight-nearest-neighbor model, with four axially symmetric conditions. The notation is that of Ref. 22.

Atomic force constants (dyn/cm)		Elastic constants (10^{12} dyn/cm^2)	
1*XX*	3865.4±67	c_{11}	0.27801
1*ZZ*	−19.9±120.3		
1*XY*	3918.6±117.6	c_{44}	0.16304
2*XX*	−1043.2±109.7		
2*YY*	71.6±66	c_{12}	0.18225
3*XX*	327.0±77.3		
3*YY*	−68.6±42.8		
3*YZ*	169.3±57.1	Constraints	
3*XZ*	124.0±24.3	8(5*ZZ*)=9(5*YY*)−5*YX*	
4*XX*	76.3±35.0	3(7*YZ*)=7*XY*	
4*ZZ*	105.7±56.5	8(5*XY*)=3(5*XX*)−3(5*YY*)	
4*XY*	−210.6±122.5	2(7*XZ*)=7*XY*	
5*XX*	−30.2±66.6		
5*YY*	−99.2±34.1		
5*ZZ*	−107.8±43.2		
5*XY*	25.9±33.3		
6*XX*	34.2±29.1		
6*YZ*	89.1±64.9		
7*XX*	−52.7±32.1		
7*YY*	104.4±37.4		
7*ZZ*	14.3±20.1		
7*YZ*	−4.7±8.3		
7*XZ*	−7.0±12.5		
7*XY*	−14.0±18.6		
8*XX*	−25.0±104.3		
8*YY*	−42.6±63.8		

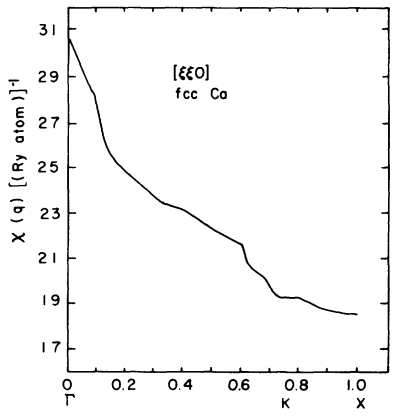

FIG. 2. Generalized susceptibility $[\chi(\vec{q})]$ for bands 1 and 2 of fcc Ca along the $[\xi\xi 0]$ direction.

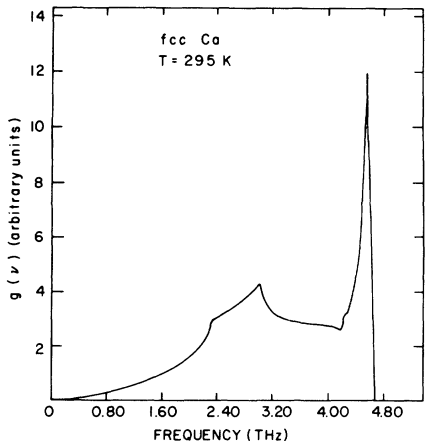

FIG. 3. Room-temperature phonon density of states $g(\nu)$ of fcc Ca, evaluated using the force constants listed in Table II.

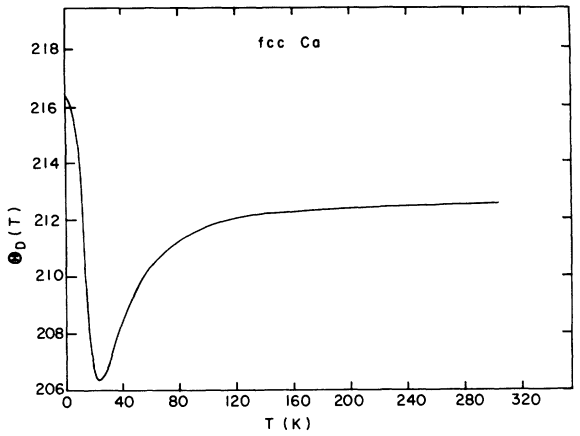

FIG. 4. Temperature dependence of the effective Debye temperature of fcc Ca, evaluated using the room-temperature phonon density of states plotted in Fig. 4.

by time-of-flight measurements on polycrystalline samples. Notice that the shear moduli c_{44} and $(c_{11}-c_{12})/2$ differ by a factor of 3.4. This observation implies strong anisotropy in the propagation of elastic waves in fcc Ca, again a result very similar to that obtained[6] for fcc Yb.

The room-temperature phonon density of states $g(\nu)$ (see Fig. 3) was calculated by the method[15] of Gilat and Raubenheimer, and it was used to evaluate the lattice specific heat as a function of temperature. The results, expressed in terms of an effective Debye temperature $\Theta_D(T)$ are plotted in Fig. 4. The 0-K Debye temperature (216.35 K) obtained in the present analysis is to be compared with the values (between 219 and 250 K) obtained by various workers[16–20] from low-temperature specific-heat measurements. The value of $\Theta_D(0)$ obtained in the present analysis seems to be somewhat lower than the average of the values obtained[16–20] from low-temperature specific-heat measurements. This is to be expected, however, since we assumed in our analysis that the phonon density of states obtained from the room-temperature phonon density of states is independent of temperature. The correction to $\Theta_D(0)$ (obtained from the room-temperature phonon spectrum), arising from the temperature dependence of the phonon frequencies, is in some cases[21] of the order of 5%.

ACKNOWLEDGMENTS

The Ames Laboratory is operated for the U. S. Department of Energy by Iowa State University under Contract No. W-7405-Eng-82; this work was supported by the Director for Energy Research, Office of Basic Energy Sciences.

*Permanent address: Risø National Laboratory, DK-4000 Roskilde, Denmark.

[1]B. Vasvari, A. O. E. Animalu, and V. Heine, Phys. Rev. B 154, 535 (1967).

[2]G. Johansen, Solid State Commun. 7, 731 (1969).

[3]G. Johansen and A. R. Mackintosh, Solid State Commun. 8, 121 (1970).

[4]J.-P. Jan and H. L. Skriver, J. Phys. F 11, 805 (1981), and references therein.

[5]U. Buchenau, H. R. Schober, and R. Wagner, J. Phys. (Paris), Colloq. 42, C6-395 (1981).

[6]C. Stassis, C.-K. Loong, C. Theisen, and R. M. Nicklow, Phys. Rev. B 26, 4106 (1982).

[7]A. O. E. Animalu, Phys. Rev. 161, 445 (1967).

[8]M. Taut and H. Eschrig, Phys. Status. Solidi B 73, 151 (1976).

[9]John A. Moriarty, Phys. Rev. B 6, 4445 (1972); 8, 1338 (1973); 16, 2537 (1977); 26, 1754 (1982).

[10]See for instance, H. Wendel and R. M. Martin, Phys. Rev. B 19, 5251 (1979); M. T. Yin and M. L. Cohen, Phys. Rev. Lett. 45, 1004 (1980); B. N. Harmon, W. Weber, and D. R. Hamann, Phys. Rev. B 25, 1109 (1982); K.-M. Ho, C. L. Fu, B. N. Harmon, W. Weber, and D. R. Hamann, Phys. Rev. Lett. 49, 673 (1982), and references therein.

[11]See for instance, M. Gupta and A. J. Freeman, in *Superconductivity in d- and f-Band Metals*, edited by D. H. Douglass (Plenum, New York, 1976), and references therein.

[12]P.-A. Lindgård, Solid State Commun. 16, 481 (1975); J. Rath and A. J. Freeman, Phys. Rev. B 11, 2109 (1975).

[13]C. M. Varma and W. Weber, Phys. Rev. B 19, 6142 (1979).

[14]U. Buchenau, Solid State Commun. 32, 1329 (1979).

[15]G. Gilat and L. J. Raubenheimer, Phys. Rev. 144, 390 (1966).

[16]P. Günther, Ann. Phys. (Leipzig) 51, 828 (1915).

[17]K. Clusius and J. V. Vaughan, J. Am. Chem. Soc. 52, 4686 (1930).

[18]L. M. Roberts, Proc. Phys. Soc. London, Sect. B 70, 738 (1957).

[19]M. Griffel, R. W. Vest, and J. F. Smith, J. Chem. Phys. 27, 1267 (1967).

[20]K. L. Agarwal and J. O. Betterton, Jr., J. Low Temp. Phys. 17, 509 (1974).

[21]C. Stassis, C.-K. Loong, and J. Zarestky, Phys. Rev. B 26, 5426 (1982).

[22]E. C. Svennson, B. N. Brockhouse, and J. M. Rowe, Phys. Rev. 155, 619 (1967).